STM JOURNALS

Journal of
Polymer & Composites

ISSN: 2321-2810 (Online)
ISSN: 2321-8525 (Print)
Volume 13, Special Issue 3, 2025
DOI (Journal): 10.37591/JoPC

https://journals.stmjournals.com/jopc

Review JoPC

Biomimicry of Eucalyptus Leaf Design for Optimization and Fabrication of Airfoil

Reeti Mukherjee[1,*], A Shashank[2], N S Achyuth Anand[3], N Kiran Kumar [4], M Vamshikrishna.[5], P Arun[6]

Abstract

Biomimicry is the practice of drawing inspiration from natural forms to solve engineering problems, which has become progressively popular for refining design efficiency and performance. This work discovers how biomimicry can be applied to airfoil design, precisely through the unique structure of Eucalyptus leaves, a concept rarely explored in airfoil profiling. The work presented here, focuses on enhancing airfoil designs by incorporating the intricate features of these leaves. The airfoil in question has a thickness of 54.3mm, a chord length of 142.5mm, and operates at a Reynolds number ranging from 3E5 to 7E5, with wind speeds between 4 and 7 meters per second. The web digitizer software uses Eucalyptus Leaf design to provide leaf structural coordinates, and then the parameters are translated into a computational model using Catia, enabling the generation of a prototype airfoil structure. In due course, the newly developed airfoil undergoes experimental testing within a wind tunnel environment to assess its aerodynamic characteristics. Factors such as lift, drag, and stall characteristics are inspected to determine how efficient the biomimetic approach is, and comparing the result to traditional airfoil designs has shown some results that need optimization of design for applications in the real world. This comprehensive approach highlights the collaboration between biological inspiration, computational models, and experimental validation in advancing aerodynamic design specimens. This study looks at how the natural design of eucalyptus leaves can inspire better air foil designs. It focuses on using advanced polymers and composite materials that replicate the leaf's strong, yet lightweight structure, while also maintaining the right balance of weight and flexibility for optimal performance.

Keywords: Biomimetic design, computational modelling, polymers, composite materials, aerodynamic performance

INTRODUCTION

The shape of the blade, known as the airfoil, greatly affects how effectively it catches the wind. it works by producing suction on the upper surface of the blade to create lift and rotate the blade, numerous organizations including NACA, NREL, and other institutes, research airfoils. Recently several airfoil[1,3] studies based on natural morphology, particularly airfoil morphology from animal movements have been produced. For instance, scientists have explored airfoil designs influenced by the swimming patterns of dolphins and the physical characteristics of sturgeon fish. Moreover, extensive research[4,6] has delved into the wing formations of avian species and dragonflies, such as the distinctive shapes seen in owls, the mechanics of bird wing flapping, and the unique wing structure of the dragonfly species Aeshna Cyanea and additionally, engineers have drawn inspiration from the streamlined shape and efficient propulsion of whale fins to develop wind turbine blades with biomimetic characteristics. Mimicking the

***Author for Correspondence**
Reeti Mukherjee

[1]Assistant Professor, Department of Mechanical engineering, ACE Engineering College, Hyderabad, Telangana, India
[2-6]Student, Department of Mechanical engineering, ACE Engineering College, Hyderabad, Telangana India

Received Date: September 13,2024
Accepted Date: April 08, 2025
Published Date: April 26, 2025

Citation: Reeti Mukherjee, A Shashank, N S Achyuth Anand, N Kiran Kumar, M Vamshi Krishna, P Arun. Biomimicry of eucalyptus leaf design for optimization and fabrication of airfoil. Journal of Polymer & Composites. 2025; 13(Special Issue 3): S359–S373p.

morphology of whale fins, such as their smooth surfaces and curved edges, these blades aim to enhance aerodynamic performance and energy capture efficiency. Incorporating features that reduce drag and turbulence, these blades operate more effectively in varying wind conditions, demonstrating a biometric approach that optimizes wind energy conversion technology. This can be further efficiently done by using different materials like polymers and composite materials.

Recent research has significantly advanced the understanding and development of bio-inspired airfoil and composite materials. Rosa et al. [1] discussed sustainable approaches in environmental engineering, setting the context for innovative airfoil research. Prof. Sahana D. S. and Prof. Srinath R. [2] designed a bio-inspired airfoil for basic aircraft, emphasizing structural adaptation from nature. Herrera et al. [3] developed and manufactured small-scale wind turbine blades using bio-inspired design principles. Huang et al. [4] proposed a dolphin-head-shaped bionic airfoil with enhanced aerodynamic performance, while Yan et al. [5] explored a novel bionic airfoil's hydrodynamic behaviour. Srividhya et al. [6] evaluated the mechanical and durability aspects of fiber-reinforced concrete using SBR latex. Tian et al. [7] analyzed the aerodynamic benefits of swallow-wing-inspired airfoils, and Hao et al. [8] conducted simulations on bionic airfoil performance. Sanket Thorwat [9] investigated lift and drag in NACA 1412 airfoils and compared wing shape influences. Achour et al.[10] developed a conditional generative adversarial network (cGAN) for optimizing airfoil shapes, while Barrett et al. [11] applied multi-fidelity analysis for efficient airfoil design. Drela [12] introduced XFOIL, a pivotal tool for analyzing low Reynolds number airfoils, and Jameson [13] demonstrated CFD-based optimization techniques in aerodynamic design. Zhao et al. [14] optimized supercritical wings through airfoil transformation methods, and Zhang et al. [15] contributed to the development of natural laminar flow airfoils for regional aircraft. Santulli et al. [16] explored the properties and applications of pineapple fiber composites. Palanisamy et al. [17] tailored epoxy composites using Acacia caesia bark fibers, examining the impact of fiber content and size. Karthik et al. [18] reviewed surface modification strategies to enhance plant fiber-based bio-composites. Palaniappan et al. [19] synthesized microcrystalline cellulose from citrus peel waste for polymer applications, and Palanisamy et al. [20] characterized Acacia caesia bark fibers for use in natural fiber composites. Collectively, these studies contribute to a broader understanding of aerodynamic performance enhancement and sustainable material integration through bio-inspiration and advanced optimization techniques.

GEOMETRIC MODELING AND NUMERICAL METHOD

Biomimetic Design Approach

This work embarks on a journey inspired by the complex structure of Eucalyptus leaves, exploring the realm of biomimicry principles to reconsider airfoil optimization and fabrication. Drawing the design from eucalyptus leaves, the airfoil profile is precisely crafted to mirror the efficiency and performance-enhancing characteristics found in this natural design. The fundamental aspect of the methodology involves a deep understanding of the natural morphology particularly found in Eucalyptus leaves, through Careful observation and computational modeling, the eucalyptus leaf design is replicated with unparalleled precision.

Computational Modeling with CATIA

Utilizing the web digitizer software, the structural coordinates extracted from Eucalyptus leaves are harnessed to construct a comprehensive computational model Figure 1(a) within CATIA software. This advanced process facilitates the translation of biomimetic design principles into a prototype airfoil structure. Leveraging the capabilities of CATIA ensures precision and accuracy in every aspect of the model, maintaining consistency in the intricate details of natural morphology Figure 1(b). The essence of biomimicry is carefully captured, making the way for transformative advancements in airfoil design.

Experimental Validation in Wind Tunnel

The 3D printed airfoil which was a design inspired by the Eucalyptus leaves underwent rigorous experimental testing which was carried out carefully in a regulated wind tunnel environment. Here, the newly developed biomimetic airfoil undergoes comprehensive evaluation, with the main focus on

aerodynamic characteristics which include lift, drag, and stall behavior. This testing enabled vital insights into the effectiveness of the biomimetic airfoil in its performance comparison to traditional airfoil design. Figure 2 shows the Testing Of 3D Printed Airfoil In Wind Tunnel

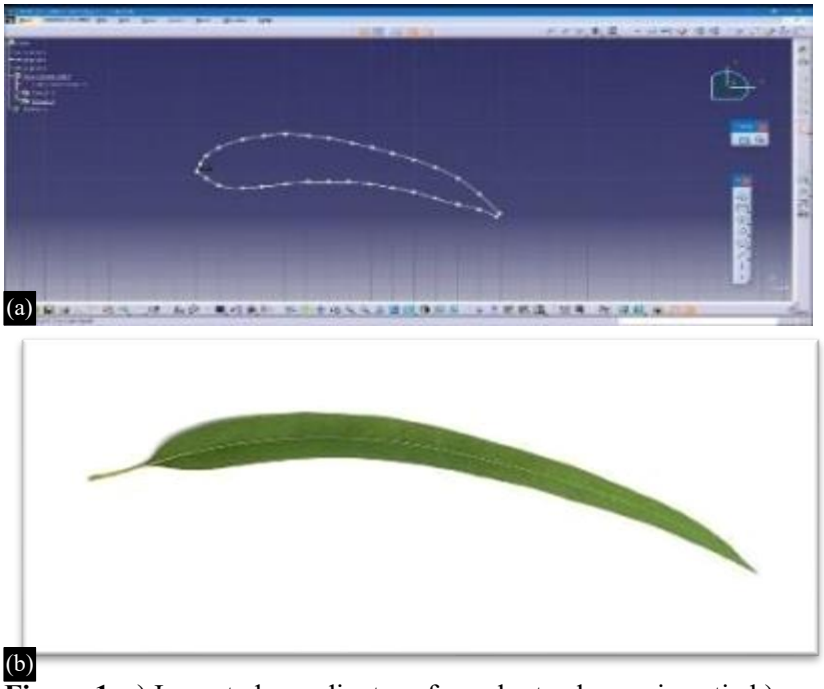

Figure 1. a) Imported coordinates of eucalyptus leaves in catia b) profile of eucalyptus leaves.

Figure 2. Testing of 3D printed airfoil in wind tunnel.

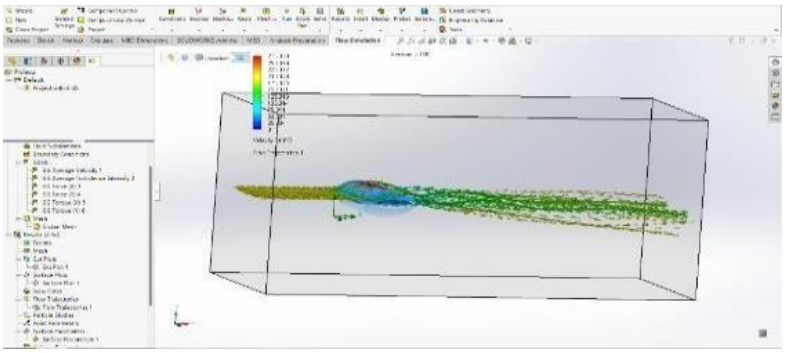

Figure 3. Flow simulation of airfoil in solid works.

Flow Simulation Analysis with SolidWorks

In tandem with physical testing, our study also includes cutting-edge flow simulation analysis utilizing SolidWorks software. Figure 3 shows the advanced computational fluid dynamics (CFD) simulation which provides a detailed understanding of the complex airflow dynamics encircling our biomimetic airfoil design. By carefully analyzing factors such as velocity distribution, pressure gradients, and turbulence patterns, a comprehensive understanding of the aerodynamic performance of our biomimetic airfoil have been obtained.

TEST RESULTS AND DISCUSSION

Extensive aerodynamic tests are conducted on the newly designed biomimetic airfoil, which is inspired by the intricate structure of eucalyptus leaves. these tests were carefully carried out under controlled atmospheric conditions in a simulation, across a range of angles of attack from -30 degrees to +16 degrees, and at varying Reynolds numbers from 3E5 to 7E5, Throughout the experiments revealed a consistent trend in the lift coefficient values across the tested range of angles. Notably the optimal aerodynamic performance was achieved at a Reynolds number of 3E5, where the maximum lift at an angles of attack 14 degree is 0.21. The airfoil functions optimally in these particular operational circumstances. For the wind tunnel tests, the maximum available wind speed of 35 m/s is utilized. The angle of attack that were chosen for a thorough analysis were the most efficient, at +16 degrees, which showed the greatest lift, and -30 degrees for a comparative analysis, representing a significantly low angle. The purpose of these selections was to assess the airfoil's performance spectrum in both ideal and difficult circumstances. It is clear from a close inspection of the data that the performance measures at certain angles +6, +9, +12, and +14 degrees—are especially promising. These findings highlight the possibility of significantly improving aerodynamic efficiency by refining the airfoil design in these settings.

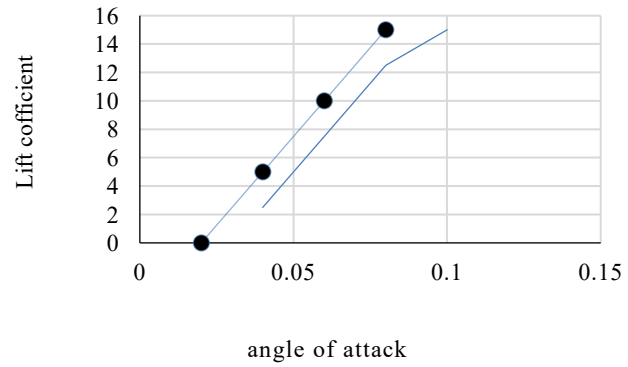

Figure 4. Lift coefficient with different angle of attack for re number 3E5.

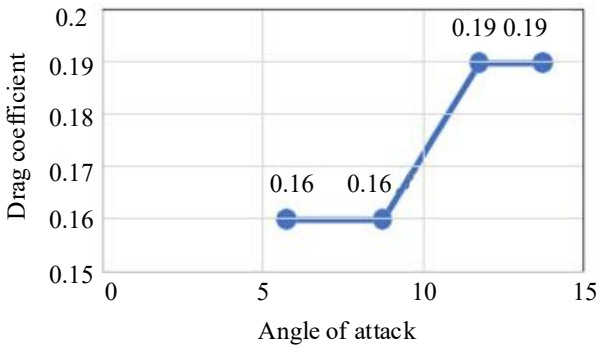

Figure 5. Drag coefficient with different angle of attack for re number 3E5.

The given graphs in Figure 4 and Figure 5 illustrate the variations in lift and drag coefficients for different angles of attack at a Reynolds number of 3E5. At an angle of attack of +6 degrees, the lift coefficient was measured at 0.09, with a corresponding drag coefficient of 0.16. Increasing the angle to +9 degrees, the lift coefficient increases to 0.14, while the drag coefficient remains steady at 0.16. Further elevation to +12 degrees resulted in a lift coefficient of 0.19 and a drag coefficient of 0.19. Notably, at +14 degrees, the lift coefficient reached its peak at 0.21, with the drag coefficient also at 0.19.

The graphs given in Figure 6 and Figure 7 illustrate the variations in lift and drag coefficients for different angle of attack at a Reynolds number of 4E5. At an angle of attack of +6 degrees, the lift coefficient was measured at 0.16, with a corresponding drag coefficient of 0.07. Increasing the angle to +9 degrees, the lift coefficient increases to 0.16 while the drag coefficient remained steady at 0.1. Further elevation to +12 degrees resulted in a lift coefficient of 0.18 and a drag coefficient of 0.12. Notably, at +14 degrees, the lift coefficient reached its peak at 0.19, with the drag coefficient also at 0.15.

The given graphs in Figure 8 and Figure 9 illustrate the variations in lift and drag coefficients for different angle of attack at a Reynolds number of 5E5. At an angle of attack of +6 degrees, the lift coefficient was measured at 0.05 with a corresponding drag coefficient of 0.16. Increasing the angle to +9 degrees, the lift coefficient increases to 0.07 while the drag coefficient remained steady at 0.15 Further elevation to +12 degrees resulted in a lift coefficient of 0.1 and a drag coefficient of 0.17. Notably, at +14 degrees, the lift coefficient reached its peak at 0.12 with the drag coefficient also at 0.17.

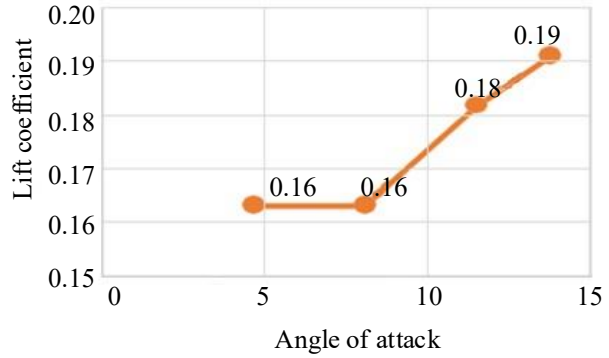

Figure 6. Lift coefficient with different angle of attack for re number 4E5.

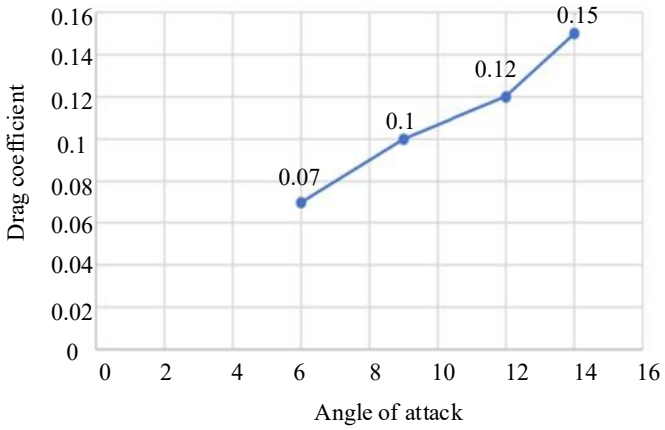

Figure 7. Drag coefficient with different angle of attack for re number 4E5.

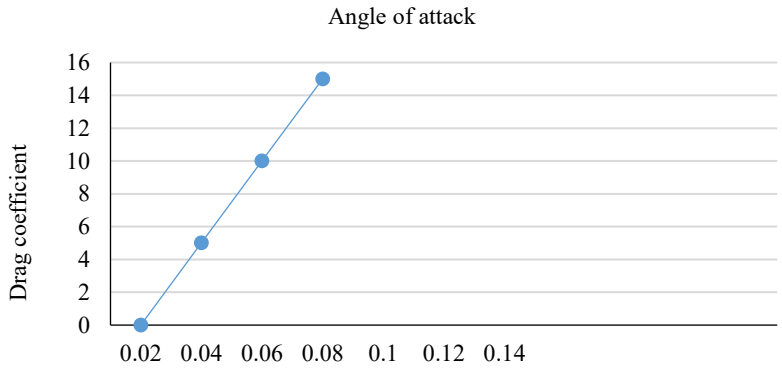

Figure 8. Lift coefficient with different angle of attack for Re number.

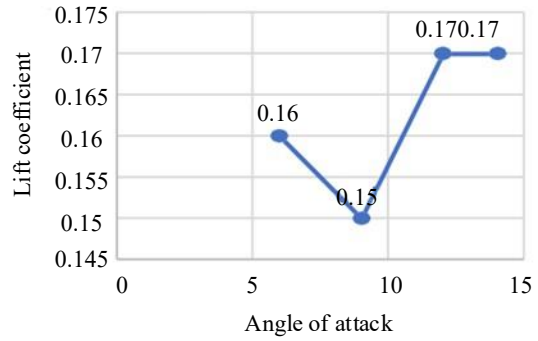

Figure 9. Drag coefficient with different angle of attack for Re number 5E5.

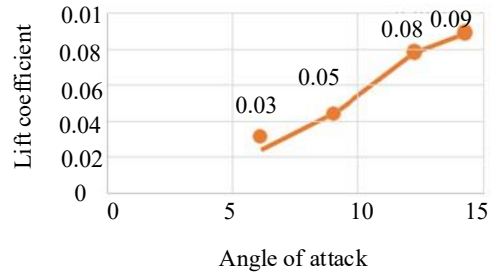

Figure 10. Lift coefficient with different angle of attack for Re number 6E5.

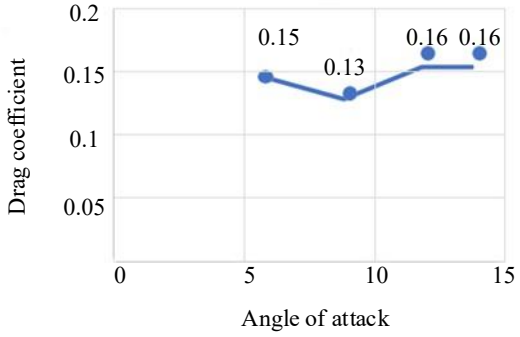

Figure 11. Drag coefficient with different angle of attack for Re number 6E5.

The given graphs in Figure 10 and Figure 1 illustrate the variations in lift and drag coefficients for different angle of attack at a Reynolds number of 6E5. At an angle of attack of +6 degrees, the lift coefficient was measured at 0.03 with a corresponding drag coefficient of 0.15. Increasing the angle to

+9 degrees, the lift coefficient increases to 0.05 while the drag coefficient remained steady at 0.13. Further elevation to +12 degrees resulted in a lift coefficient of 0.08 and a drag coefficient of 0.16 Notably, at +14 degrees, the lift coefficient reached its peak at 0.09 with the drag coefficient also at 0.16.

The given graphs in Figure 12 and Figure 13 illustrate the variations in lift and drag coefficients for different angles of attack at a Reynolds number of 6E5. At an angle of attack of +6 degrees, the lift coefficient was measured at 0.02 with a corresponding drag coefficient of 0.14. Increasing the angle to +9 degrees, the lift coefficient increased to 0.04 while the drag coefficient remained steady at 0.12 Further elevation to +12 degrees resulted in a lift coefficient of 0.07 and a drag coefficient of 0.14 Notably, at +14 degrees, the lift coefficient reached its peak at 0.08 with the drag coefficient also at 0.15.

PRESURE AND VELOCITY

Figure 14-23 depict the airflow at various Reynolds numbers. In general, the airflow velocity around the surface of the airfoil is 0 m/s. The separation, however, decreases as the Reynolds number increases. The airflow velocity varies on the top and bottom surfaces of the airfoil, with the top surface having a higher velocity than the bottom surface. High airflow velocity, according to Bernoulli's principle, leads to reduced surface pressure. As a result, the upper surface pressure of the airfoil with Reynolds numbers 3E5 to 7E5 is lower than the lower surface pressure, allowing the airfoil to generate lift more effectively.

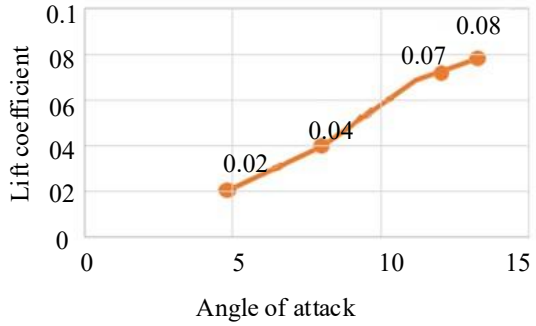

Figure 12. Lift coefficient with different angle of attack for Re number 7E5.

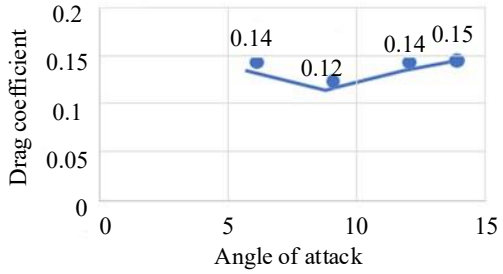

Figure 13. Drag coefficient with different angle of attack for Re number 7.

Table 1. Experiment Results.

Angle of attack	Lift coefficient (CI)	Drag coefficient (Cd)	Pitching moment coefficient (Cm)	CI/Cd ratio
-35	0.23	0.54	0.09	0.42
-24	0.04	0.42	0.13	0.09
-18	-0.02	0.34	0.18	-0.05
0	-0.34	0.22	0.14	-1.54
9	-0.05	0.27	0.10	-0.18

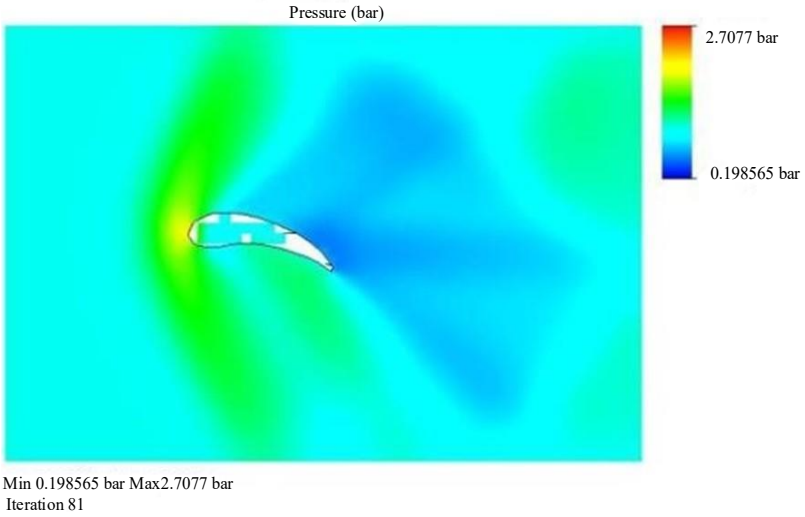

Figure 14. Comparison of pressure contours of airfoil at different angle of attack and reynolds number 3E5.

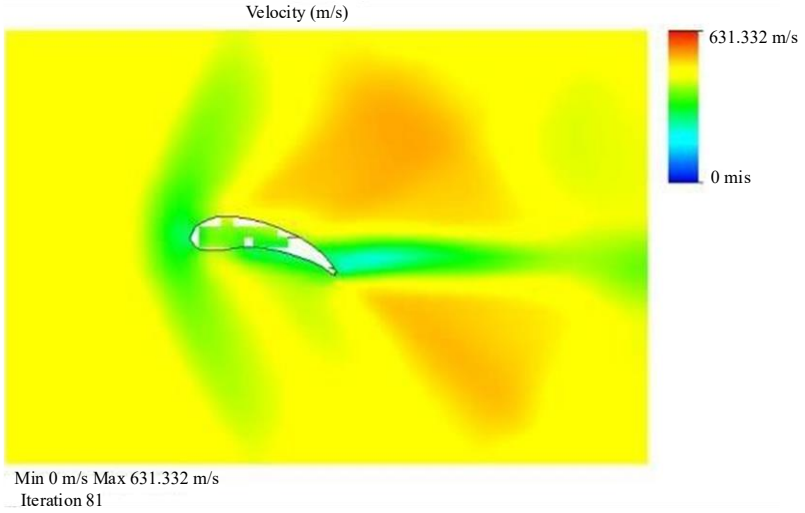

Figure 15. Comparison of velocity contours of airfoil at different angle of attack and Reynolds number 3E5.

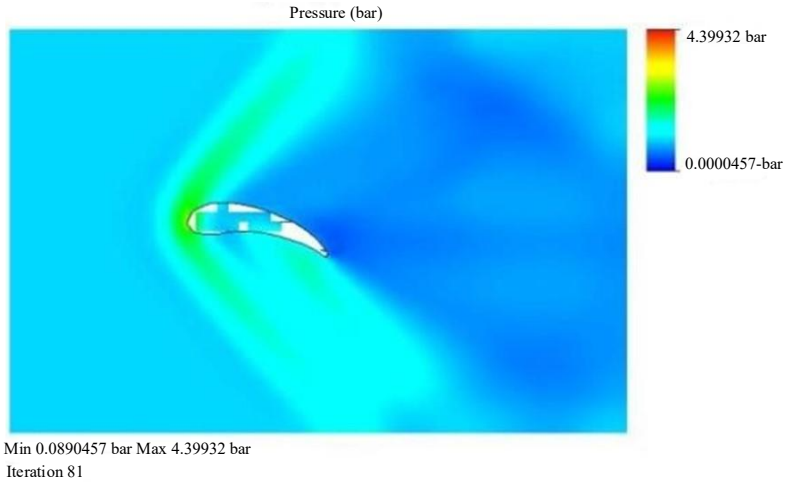

Figure 16. Comparison of pressure contours of airfoil at different angle of attack and Reynolds number 4E5.

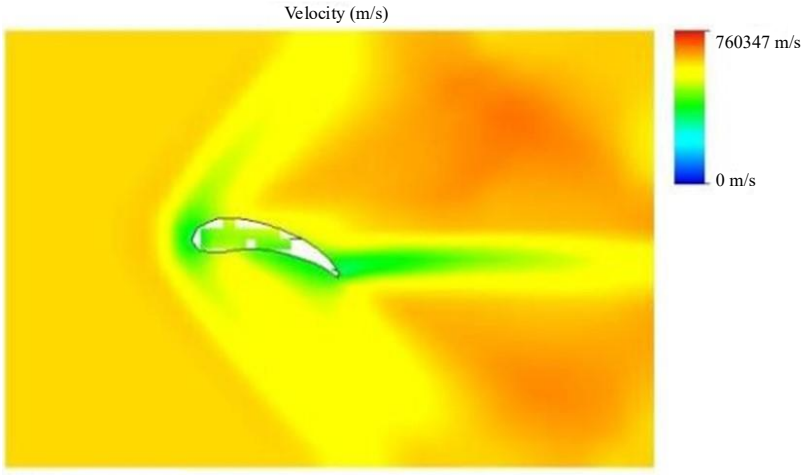

Figure 17. Comparison of velocity contours of airfoil at different angle of attack and reynolds number 4E5

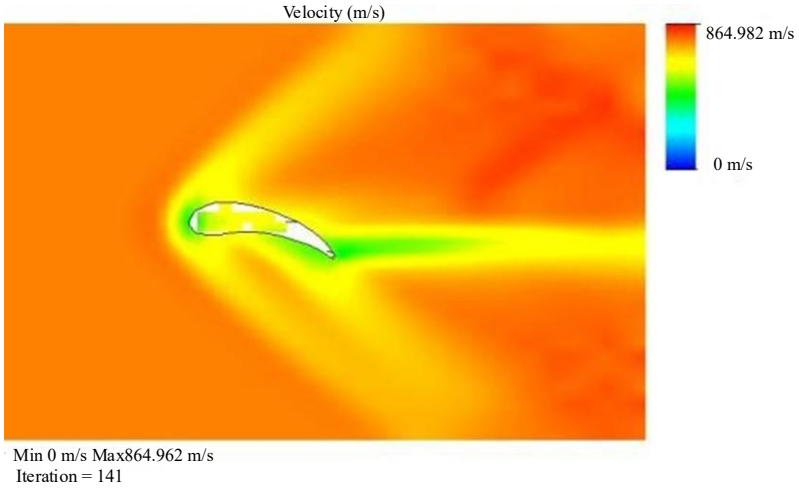

Figure 18. Comparison of pressure contours of airfoil at different angle of attack and Reynolds number 5E5

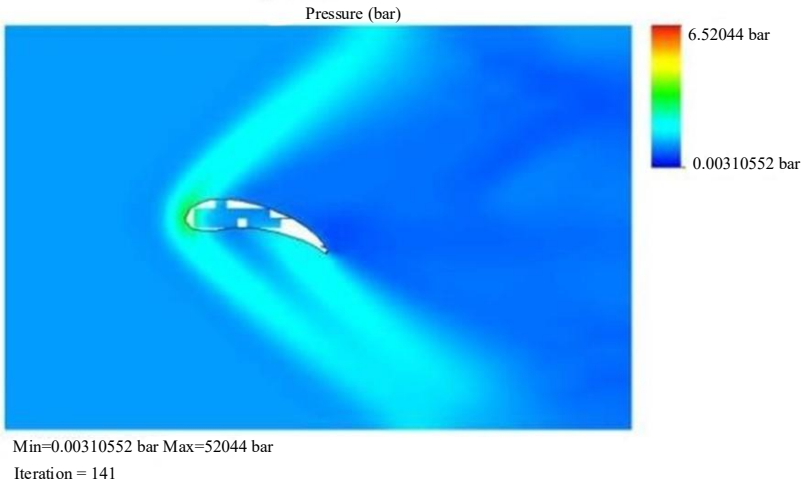

Figure 19. Comparison of velocity contours of airfoil at different angle of attack and Reynolds number 5E5.

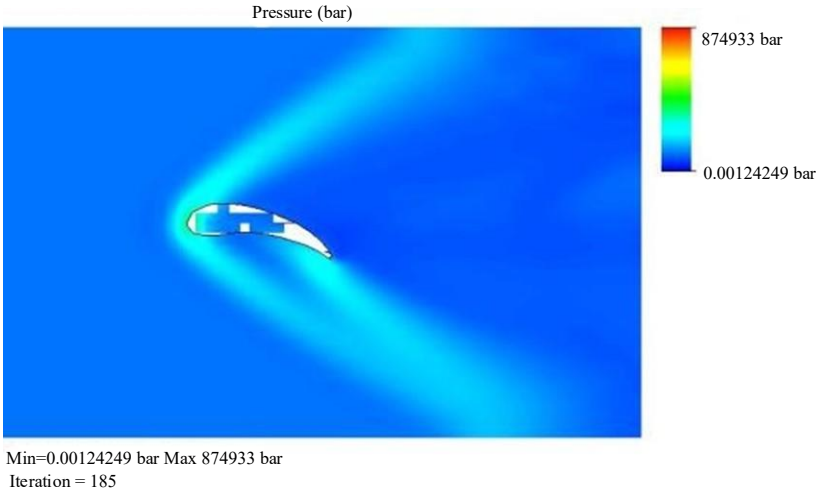

Figure 20. Comparison of pressure contours of airfoil at different angle of attack and Reynolds number 6E5.

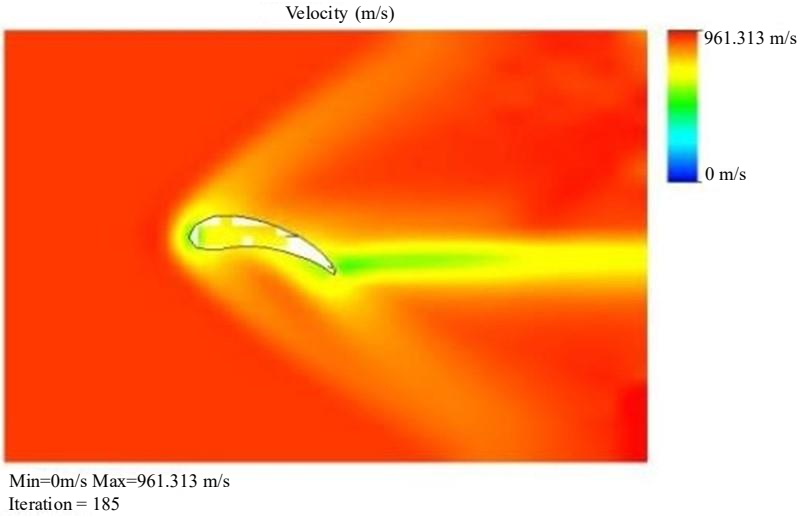

Figure 21. Comparison of velocity contours of airfoil at different angle of attack and Reynolds number 6E5.

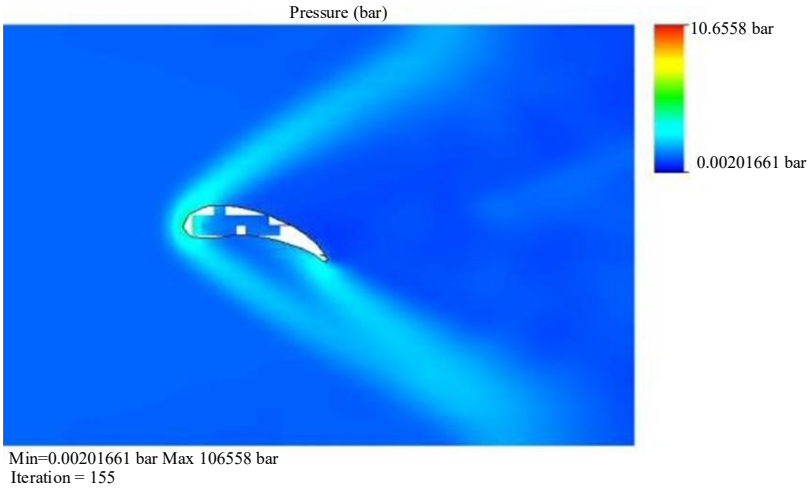

Figure 22. Comparison of pressure contours of airfoil at different angle of attack and Reynolds number 7E5

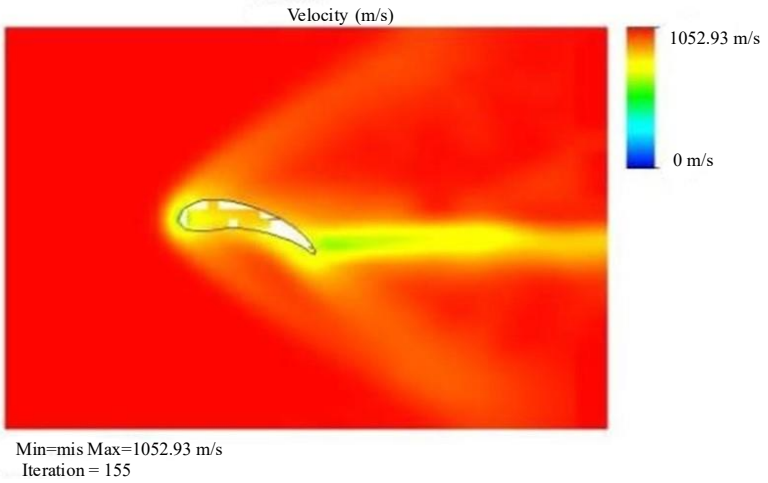

Figure 23. Comparison of velocity contours of airfoil at different angle of attack and Reynolds number 7E5.

COMPARISON OF EUCALYPTUS LEAF DESIGN AIRFOIL WITH NACA 6409

The NACA 6409 is an airfoil with a set of specific characteristics optimized for aerodynamic performance. At 29.3% chord, its maximum thickness is 9%, while at 39.6% chord, its maximum camber is 6%, This design is part of the NACA (National Advisory Committee for Aeronautics) airfoil series, which are shapes for aircraft wings developed to increase lift and reduce drag. The NACA 6409 airfoil is particularly noted for its use in free-flight model planes rather than radio-controlled (RC) soaring. In terms of aerodynamic performance, the thickness and camber of the airfoil significantly influence on its behavior, and there's a strong dependence on the Reynolds number. For example, a Reynolds number of 50,000 and a critical pressure coefficient (NCRIT) of 9, the maximum lift- to-drag ratio (Cl/Cd) is 27.1 at an angle of attack (α) of 10.75°1. These characteristics make the NACA 6409 suitable for specific aerodynamic applications where such performance metrics are critical. Lift and Drag coefficients of NACA 6409 are obtained by conducting flow simulation in SolidWorks. The data of NACA 6409 is compared with Biomimicry design airfoil (EU14). The Comparison of The Lift Coefficient Of The Biomimicry Design Airfoil with NACA 6409 At A Velocity Of 126km/H. is shown in Figure 24.

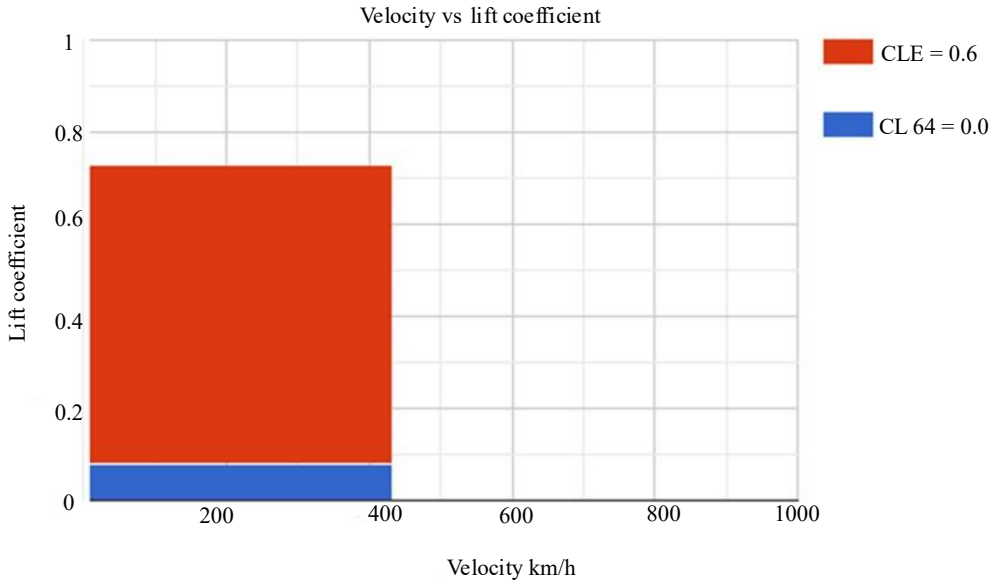

Figure 24. Comparison of the lift coefficient of the biomimicry design airfoil with NACA 6409 At A Velocity Of 126km/H.

The Comparison of The Lift Coefficient Of The Biomimicry Design Airfoil with NACA 6409 At A Velocity Of *860km* /H. is shown in Figure 25.

Comparison Of The Drag Coefficient Of Biomimicry Design Airfoil With NACA 6409 At A Velocity Of 126km/H is shown in Figure 26.

Comparison Of the Drag Coefficient of Biomimicry Design Airfoil With NACA 6409 At A Velocity Of 860Km/H is shown in Figure 27.

Comparison Of the C_l/C_d Ratio of Biomimicry Design Airfoil with NACA 6409 At A Velocity Of 860Km/H is shown in Figure 28.

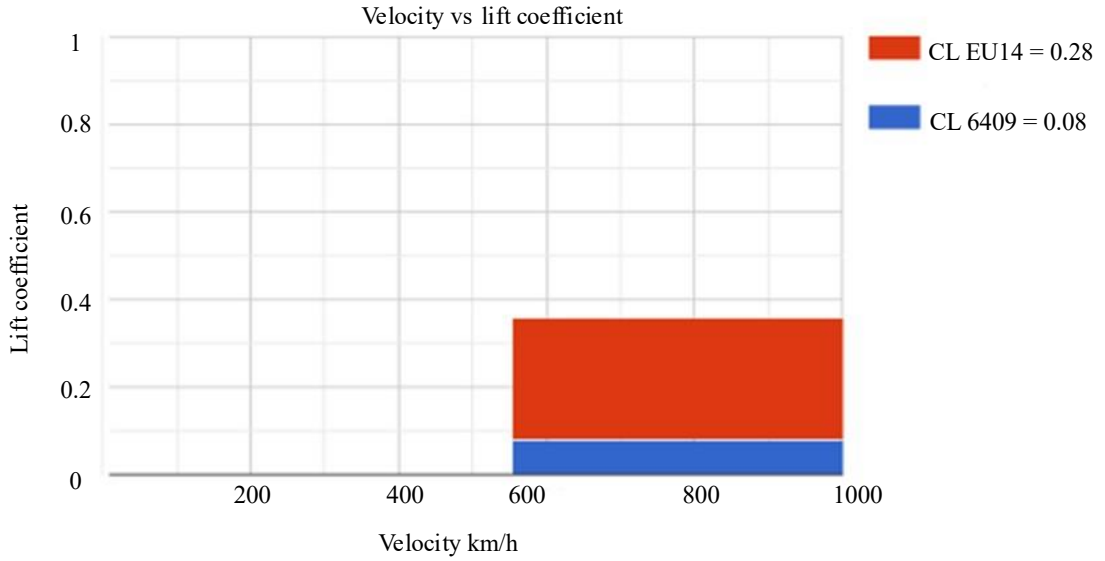

Figure 25. Comparison of the lift coefficient of biomimicry design airfoil with NACA 6409 At A Velocity Of 860km/H.

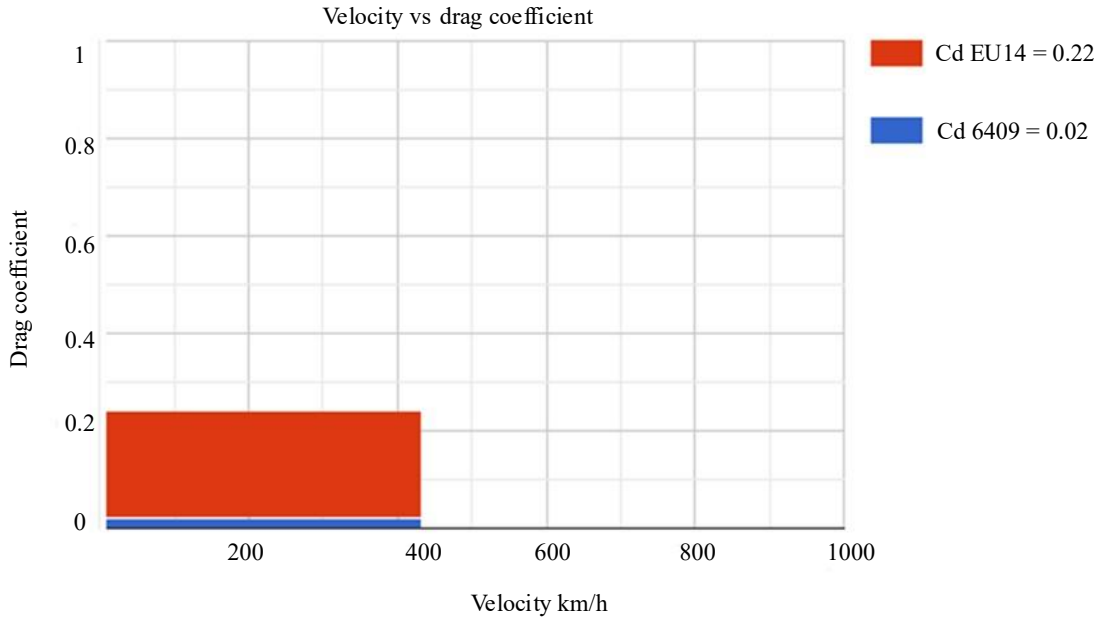

Figure 26. Comparison of the drag coefficient of biomimicry design airfoil with NACA 6409 At A Velocity Of 126km/H.

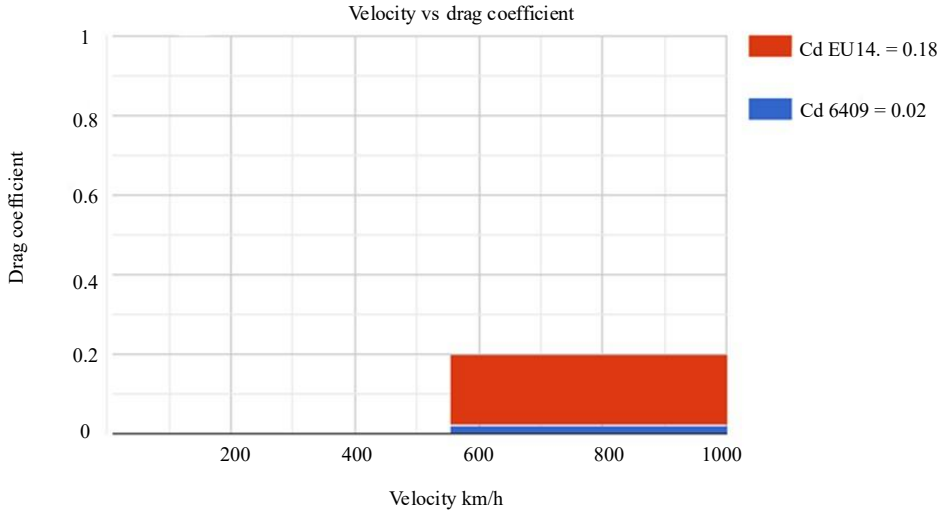

Figure 27. Comparison of the drag coefficient of biomimicry design airfoil with NACA 6409 At A Velocity Of 860km/H.

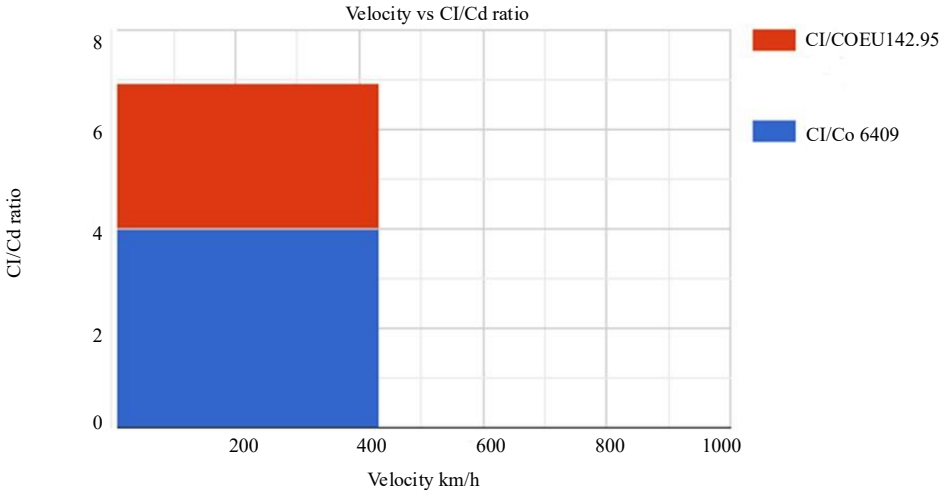

Figure 28. Comparison of the Cl/Cd Ratio of Biomimicry Design Airfoil with NACA 6409 At A Velocity Of 126km/H.

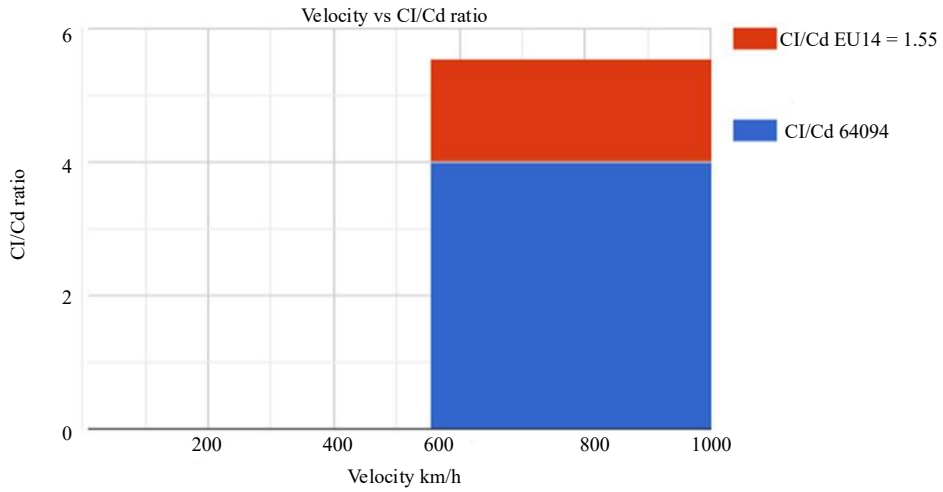

Figure 29. Comparison Of the C_l/C_d Ratio of Biomimicry Design Airfoil With NACA 6409 At A Velocity Of 860km/H.

Comparison Of The C_l/C_d Ratio of Biomimicry Design Airfoil with NACA 6409 At A Velocity Of 860Km/H is shown in Figure 29.

CONCLUSION

Based on the findings and analysis this study has promising potentials of biomimicry in advance airfoil design for wind energy application. Biomimetic airfoil is created by emulating the complicated structure of Eucalyptus leaves, which has improved aerodynamic performance. The combination of computational modeling, experimental validation, and CFD simulations has provided valuable insights into the behavior of the biomimetic airfoil, highlighting its competitive advantage over standard design.

Moving forward, additional optimization and refinement hold the key of unlocking the full potential of biomimetic airfoil. By taking cues from the leaf's aerodynamic shape, efficient structure, and ability to adapt, airfoils made from advanced polymers and composites can perform better, offering reduced drag, increased lift, and overall greater efficiency. The combination of lightweight, strong materials with the potential for dynamic adaptability could significantly enhance airfoil performance in a wide range of conditions. As this bio-inspired approach continues to evolve, it has the potential to provide more sustainable, effective solutions for both aerospace and renewable energy fields, advancing the possibilities of material science and aerodynamic design.

REFERENCES

1. F Rosa *et al* 2022 *IOP Conf. Ser.: Earth Environ. Sci.* 1108 012001
2. Prof. Sahana D S, Prof. Srinath R ,"Bio-Inspired Study and Build-Out of New Airfoil for the Design of Basic Aircraft ", Volume. 2 Issue. 11, November- 2017, *International Journal of Innovative Science and Research Technology (IJISRT)* , www.ijisrt.com, ISSN - 2456-2165, PP:-180-187.
3. Camilo Herrera, Mariana Correa, Valentina Villada, Juan D. Vanegas, Juan G. García, César Nieto-Londoño, Julián Sierra-Pérez, Structural design and manufacturing process of a low scale bio-inspired wind turbine blades, *Composite Structures*, Volume 208, 2019, Pages 1-12, ISSN 0263-8223.
4. Shengxian Huang, Yu Hu, Ying Wang, Research on aerodynamic performance of a novel dolphin head-shaped bionic airfoil, *Energy,* Volume 214, 2021, 118179, ISSN 0360-5442,
5. Yan H, Su X, Zhang H, Hang J, Zhou L, Liu Z and Wang Z 2020 Design approach and hydrodynamic characteristics of a novel bionic airfoil Ocean Eng. 216 108076 Xinyu L, Bifeng S, Wenqing Y and Wenping S 2021 Aerodynamic performance of owl-like
6. S. Srividhya, R. Prakash, M. Vinod Kumar, et.al, 2024, Impact of various Fibers on the Mechanical and Durability Performance of Fibre-Reinforced Concrete with SBR latex, Journal of Polymer & Composites, Vol 12, No 2, 2024
7. Tian, Weijun & Liu, Fangyuan & Cong, Qian et.al (2014). Study on aerodynamic performance of the bionic airfoil based on the swallow's wing. *Journal of Mechanics in Medicine and Biology*. 13. 10.1142/S0219519413400228.
8. Hao, Lishu & Gao, Yongwei & Wei, Binbin & Song, Ke. (2021). Numerical Simulation of Flow over Bionic Airfoil. *International Journal of Aerospace Engineering*. 2021. 1-17. 10.1155/2021/5556463.
9. Sanket Thorwat Lift and Drag Analysis of NACA 1412 Airfoil Using Unstructured Mesh Influence of Wing Shape on Airfoil Performance: a Comparative Study. *International Journal For Research in Applied Science and Engineering Technology.* 2013.
10. Achour G, Sung WJ, Pinon- Fischer OJ, et al. Development of a conditional generative adversarial network for airfoil shape optimization.*Aerospace research centre. 2020.*
11. Barrett TR, Bressloff NW, Keane AJ (2006) Airfoil shape design and optimization using multifidelity analysis and embedded inverse design. AIAA J 44(9):2051–2060
12. Drela, Mark. (1989). XFOIL: An Analysis and Design System for Low Reynolds Number Airfoils. 54. 10.1007/978-3-642-84010-4_1. *Conference on Low Reynolds Number Airfoil Aerodynamics, University of Notre Dame.*

13. Jameson, Antony. (1995). Optimum Aerodynamic Design Using CFD And Control Theory. CFD Review. 3. 10.2514/6.1995-1729. *12th Computational fluid dynamics conference, 1995*
14. Tong Zhao, Yufei Zhang, Haixin Chen, et al., Supercritical wing design based on airfoil optimization and 2.75D transformation,*Aerospace Science and Technology*,Volume 56,2016,Pages 168-182,ISSN 1270-9638,
15. Zhang Y, Fang X, Chen H, et al. (2015) Supercritical natural laminar flow airfoil optimization for regional aircraft wing design. *Aerospace Science and Technology* 43:152–164.
16. Carlo Santulli, Sivasubramanian Palanisamy, Mayandi Kalimuthu, Chapter 14 - Pineapple fibers, their composites and applications, Editor(s): Sanjay Mavinkere Rangappa, Jyotish Kumar Parameswaran Pillai, Suchart Siengchin, Togay Ozbakkaloglu, Hao Wang, In The Textile Institute Book Series, Plant Fibers, their Composites, and Applications, Woodhead Publishing, 2022, Pages 323-346, ISBN 9780128245286.
17. Palanisamy, S.; Kalimuthu, M.; Santulli, C.; Palaniappan, M.; Nagarajan, R.; Fragassa, C. Tailoring Epoxy Composites with *Acacia caesia* Bark Fibers: Evaluating the Effects of Fiber Amount and Length on Material Characteristics. *Fibers* 2023, *11*, 63. https://doi.org/10.3390/fib11070063
18. JOUR Karthik, A. Bhuvaneshwaran, M. Senthil Kumar, M. S. Palanisamy, Sivasubramanian Palaniappan, Murugesan Ayrilmis, Nadir e202400650 A Review on Surface Modification of Plant Fibers for Enhancing Properties of Biocomposites ChemistrySelect 9 ISSN - 2365-6549.
19. Palaniappan, M., Palanisamy, S., Khan, R. *et al.* Synthesis and suitability characterization of microcrystalline cellulose from *Citrus* x *sinensis* sweet orange peel fruit waste-based biomass for polymer composite applications. *J Polym Res* 31, 105 (2024). https://doi.org/10.1007/s10965-024-03946-0
20. Palanisamy, S., Kalimuthu, M., Palaniappan, M., Alavudeen, A., Rajini, N., Santulli, C. Al-Lohedan, H. (2021). Characterization of *Acacia caesia* Bark Fibers (ACBFs). *Journal of Natural Fibers*, *19*(15), 10241–10252. https://doi.org/10.1080/15440478.2021.1993493.

